# Infrared intensities of amide modes in *N*-methylacetamide and poly(glycine I) from *ab initio* calculations of dipole moment derivatives of *N*-methylacetamide[a)]

T. C. Cheam and S. Krimm
*Biophysics Research Division, University of Michigan, Ann Arbor, Michigan 48109*

(Received 7 June 1984; accepted 7 September 1984)

The infrared intensities of the amide modes in *N*-methylacetamide (NMA) and poly(glycine I) (PGI) have been studied using *ab initio* dipole moment derivatives obtained for the peptide group in NMA and an empirical force field refined for PGI. Good agreement is found between the calculated transition moment magnitudes and directions of the amide I and II modes and experimental intensity and dichroism data. By analyzing the separate contributions of each internal coordinate to the total intensity, we are able to understand in detail the origins of the IR intensities of the amide modes. Besides demonstrating one approach by which IR intensities can be studied in complex molecules and polymers, our results also provide a basis for using IR intensities in structural studies of peptides and polypeptides.

## INTRODUCTION

Much progress has been made recently in the theoretical study of infrared (IR) intensities.[1] It is becoming increasingly feasible to account quantitatively for observed intensities, particularly in simple molecules and highly symmetric polymers. For peptides and polypeptides, however, comparatively little attention has been paid to the calculation of IR intensities.[2] In recent years, we have developed valence force fields for polypeptides and demonstrated their high predictive capability for vibrational frequencies.[3] It is now appropriate to try as well to calculate intensities in order to enhance the validity and usefulness of normal mode calculations in structural studies of peptides and polypeptides.

Our goal is to derive a set of transferable parameters that, together with our empirical force fields, will yield reasonably reliable intensities of the amide modes. Because of the low symmetry of peptides, it would be extremely difficult to determine an accurate set of bond moment (electro-optical) parameters[1] from experimental intensity data. Our procedure, described in this paper, is first to calculate by *ab initio* Hartree–Fock methods the dipole moment derivatives $\partial\mu/\partial S_i$ with respect to the local symmetry internal coordinates of the amide group in *N*-methylacetamide (NMA); this is done for an isolated NMA molecule and for a model system of NMA hydrogen bonded to two formamide molecules. The results are then compared with experimental data for NMA. In order to transfer these dipole derivatives to polypeptides, we invoke the group moment model used successfully by Snyder[4] for *n*-paraffins. We test the transferability of the group moment derivatives by comparing with data on poly(glycine I). In future work we will examine other peptides and polypeptides; we also hope to do similar calculations on other model compounds such as amino acids to get the dipole derivatives for side chain groups.

[a)] This is paper No. 26 in a series on *Vibrational Analysis of Peptides, Polypeptides, and Proteins*. Paper No. 25 is Ref. 29.

## CALCULATIONS

For the undistorted NMA geometry, we chose the electron diffraction structure of Kitano *et al.*[5] with the angles in the methyl groups modified to tetrahedral values. The bond lengths (in Å) and angles (in degrees) are as follows ("standard" peptide unit dimensions[6] in parentheses): CC = 1.520 (1.53), NC (carbonyl) = 1.386 (1.32), NC (methyl) = 1.469 (1.47), CO = 1.225 (1.24), NH = 1.002 (1.00), CH = 1.107, CCN = 114.1 (114), CNC = 119.7 (123), NCO = 121.8 (125), HNC (carbonyl) = 110 (123). Except for the HNC angle, the experimental structure is in good agreement with a recent *ab initio* optimized geometry.[7]

To obtain the dipole derivatives when both the CO and NH groups participate in hydrogen bonds, necessary for studies of peptides in condensed states, we chose as a model system NMA complexed to two formamide molecules (Fig. 1). The formamide structure was the theoretical one obtained by Sugawara *et al.*[8] using the 4-31G basis set. The NH···OC group was taken to be linear, with an H···O distance of 1.85 Å, and the complex has planar symmetry. We note that a linear hydrogen bond may not be the best approximation to actual structures.[9]

The derivatives were calculated by displacing the atoms along S, the local symmetry internal coordinates of the CCONHC group. Table I lists these S coordinates; for brevity, the internal coordinates for the methyl groups and formamide are not shown. The positive directions of the out-of-plane bends and the torsion coordinates are defined as in Ref. 10. The Cartesian axes are oriented as in Fig. 1, with $X$ along $C_2 \rightarrow N$. Cartesian displacements corresponding to each internal coordinate distortion and satisfying the Eckart conditions were obtained by[11] $\mathbf{X} = A\,\mathbf{S}$ where $A = M^{-1}\tilde{B}(BM^{-1}\tilde{B})^{-1}$; $B$ is defined by $\mathbf{S} = B\,\mathbf{X}$ and $M$ is the matrix of atomic masses. The derivatives were evaluated by numerical differentiation: $\Delta\mu/\Delta S_i = [\mu(\Delta S_i = \Delta_i) - \mu(\Delta S_i = -\Delta_i)]/2\Delta_i$ for NMA, and $\Delta\mu/\Delta S_i = [\mu(\Delta S_i = \Delta_i) - \mu(\Delta S_i = 0)]/\Delta_i$ for the complex. Bonds were distorted by $\pm 0.01$ Å and angles by $\pm 0.025$ rad.

 0021-9606/85/041631-11$02.10  

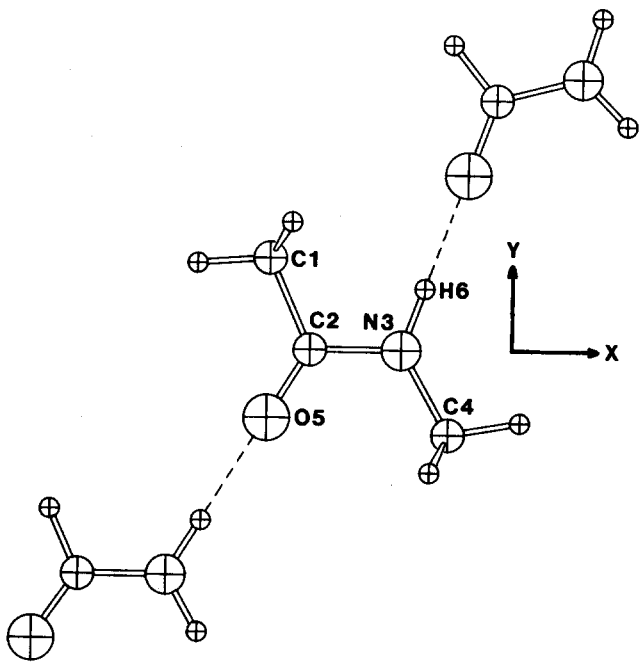


FIG. 1. Structure of *N*-methylacetamide-formamide complex used in *ab initio* calculations.

We used a version of the GAUSSIAN76 program system[12] that we further modified to run on a VAX 11/780. Because of the well-known basis set dependence of dipole moments and dipole derivatives, we tested several standard basis sets on formaldehyde, formamide, and NMA. The results for the static dipole moment $\mu_0$ and the derivative $\partial\mu/\partial r_{CO}$ are shown in Table II, together with some gas-phase experimental data. The reference geometry for formaldehyde was the optimized one for each basis[13,14]; that for formamide was the 4-31G geometry[8]; the experimental structure was used for NMA.[5] We see that the minimal STO-3G set underestimates $\mu_0$ and $\partial\mu/\partial r_{CO}$, while the 4-31G and 6-31G sets significantly overestimate these quantities. The 3-21G set[14] is clearly the best, consistently giving values between those of the smaller and larger bases.

We computed dipole derivatives for the NMA monomer using both the STO-3G and 3-21G basis sets. For the NMA-formamide complex, we used only the STO-3G set. Then, using the STO-3G results, we scaled the 3-21G derivatives for NMA to what may be expected to be 3-21G derivatives for the complex as follows: $(3\text{-}21G)_{complex} = (3\text{-}21G)_{monomer} \times [(STO\text{-}3G)_{complex}]/[(STO\text{-}3G)_{monomer}]$. Only the magnitudes were scaled; the directions of the derivatives were kept the same as the 3-21G monomer values. Hence-

TABLE I. Local symmetry coordinates of the peptide group.[a]

| | |
|---|---|
| $S_1 = \Delta r(CC)$ | CC stretch |
| $S_2 = \Delta r(C_2N)$ | CN stretch |
| $S_3 = \Delta r(NC_4)$ | NC stretch |
| $S_4 = \Delta r(CO)$ | CO stretch |
| $S_5 = \Delta r(NH)$ | NH stretch |
| $S_6 = [2\Delta\theta(CCN) - \Delta\theta(CCO) - \Delta\theta(NCO)]/\sqrt{6}$ | CCN deformation |
| $S_7 = [\Delta\theta(CCO) - \Delta\theta(NCO)]/\sqrt{2}$ | CO in-plane bend |
| $S_8 = [2\Delta\theta(CNC) - \Delta\theta(C_2NH) - \Delta\theta(C_4NH)]/\sqrt{6}$ | CNC deformation |
| $S_9 = [\Delta\theta(C_2NH) - \Delta\theta(C_4NH)]/\sqrt{2}$ | NH in-plane bend |
| $S_{10} = \Delta\omega(CO)\sin(CCN)$ | CO out-of-plane bend[b] |
| $S_{11} = \Delta\omega(NH)\sin(CNC)$ | NH out-of-plane bend[c] |
| $S_{12} = [\Delta\tau(CCNC) + \Delta\tau(CCNH) + \Delta\tau(OCNC) + \Delta\tau(OCNH)]/4$ | CN torsion |

[a] Atoms numbered as in Fig. 1.
[b] Positive: C moves in $+Z$.
[c] Positive: N moves in $-Z$.

TABLE II. Static dipole moment (in D) and derivative with respect to CO stretch (in D/Å) using various basis sets.

| Basis set | Formaldehyde | | Formamide | | *N*-methylacetamide | |
|---|---|---|---|---|---|---|
| | $\mu_0$ | $\frac{\partial\mu}{\partial r_{CO}}$ | $\mu_0$ | $\frac{\partial\mu}{\partial r_{CO}}$ | $\mu_0$ | $\frac{\partial\mu}{\partial r_{CO}}$ |
| STO-3G | 1.537 | 1.460 | 2.833 (36.9°)[a] | 3.508 | 2.721 | 3.476 |
| 3-21G | 2.658 | 3.850 | 4.149 (40.1°) | 5.996 | 3.890 | 5.576 |
| 4-31G | 3.020 | 4.435 | 4.470 (41.3°) | 6.678 | 4.215 | 6.302 |
| 6-31G | 3.042 | 4.505 | 4.512 (41.2°) | 6.791 | 4.252 | 6.686 |
| Expt. | 2.332[b] | 3.741[c] | 3.71[d] (39.6°) | | 3.71[e] | |

[a] Angle to CN bond.
[b] B. Fabricant, D. Krieger, and J. S. Muenter, J. Chem. Phys. **67**, 1576 (1977).
[c] T. Nakanaga, S. Kondo, and S. Saeki, J. Chem. Phys. **76**, 3860 (1982).
[d] R. J. Kurland and E. B. Wilson, Jr., J. Chem. Phys. **27**, 585 (1957).
[e] R. M. Meighan and R. H. Cole, J. Phys. Chem. **68**, 503 (1964).

TABLE III. Dipole derivatives $\partial\mu/\partial S_i$ (in D/A or D/rad) for NMA and NMA-formamide complex.

| | $\frac{\partial\mu_x}{\partial S}$ | $\frac{\partial\mu_y}{\partial S}$ | $\frac{\partial\mu_z}{\partial S}$ | $\left\lvert\frac{\partial\mu}{\partial S}\right\rvert$ | $\theta^a$ |
|---|---|---|---|---|---|
| STO-3G for NMA | | | | | |
| CC str | 0.555 | −0.420 | | 0.696 | −37.1 |
| CN str | −3.710 | −0.415 | | 3.733 | 6.4 |
| NC str | 1.075 | −1.825 | | 2.118 | −59.5 |
| CO str | 2.645 | 2.255 | | 3.476 | 40.4 |
| NH str | 0.500 | 0.410 | | 0.647 | 39.4 |
| CCN def | −0.495 | −0.077 | | 0.501 | 8.9 |
| CO ib | −1.741 | 1.170 | | 2.097 | −33.9 |
| CNC def | 0.620 | 0.005 | | 0.620 | 0.4 |
| NH ib | 0.216 | 0.116 | | 0.246 | 28.2 |
| CO ob | | | 0.456 | 0.456 | |
| NH ob | | | 1.695 | 1.695 | |
| CN tor | | | −0.044 | 0.044 | |
| STO-3G for NMA-formamide complex | | | | | |
| CC str | 0.520 | −0.490 | | 0.714 | −43.3 |
| CN str | −4.600 | −0.385 | | 4.616 | 4.7 |
| NC str | 1.110 | −1.770 | | 2.089 | −57.9 |
| CO str | 3.220 | 2.730 | | 4.222 | 40.3 |
| NH str | 1.160 | 1.230 | | 1.691 | 46.7 |
| CCN def | −0.365 | −0.238 | | 0.436 | −33.1 |
| CO ib | −1.123 | 0.880 | | 1.426 | −38.1 |
| CNC def | 0.238 | 0.047 | | 0.242 | 11.1 |
| NH ib | 0.289 | 0.240 | | 0.376 | 39.8 |
| CO ob | | | 0.145 | 0.145 | |
| NH ob | | | 1.515 | 1.515 | |
| CN tor | | | −0.624 | 0.624 | |
| 3-21G for NMA | | | | | |
| CC str | 0.460 | −0.540 | | 0.706 | −49.9 |
| CN str | −3.715 | −0.150 | | 3.718 | 2.3 |
| NC str | 1.380 | −2.550 | | 2.897 | −61.7 |
| CO str | 3.800 | 4.080 | | 5.575 | 47.0 |
| NH str | 0.340 | 0.615 | | 0.703 | 61.1 |
| CCN def | −0.924 | 0.044 | | 0.917 | −4.0 |
| CO ib | −2.386 | 1.705 | | 2.933 | −35.6 |
| CNC def | 1.352 | −0.196 | | 1.373 | −7.7 |
| NH ib | 0.537 | 0.109 | | 0.548 | 11.4 |
| CO ob | | | 0.451 | 0.451 | |
| NH ob | | | 2.017 | 2.017 | |
| CN tor | | | −0.272 | 0.272 | |
| 3-21G for NMA-formamide complex | | | | | |
| CC str | 0.475 | −0.558 | | 0.732 | −49.9 |
| CN str | −4.608 | −0.186 | | 4.611 | 2.3 |
| NC str | 1.366 | −2.523 | | 2.869 | −61.7 |
| CO str | 4.739 | 5.088 | | 6.953 | 47.0 |
| NH str | 0.909 | 1.644 | | 1.878 | 61.1 |
| CCN def | −0.748 | 0.036 | | 0.748 | −4.0 |
| CO ib | −1.624 | 1.161 | | 1.997 | −35.6 |
| CNC def | 0.530 | −0.077 | | 0.536 | −7.7 |
| NH ib | 0.961 | 0.195 | | 0.980 | 11.4 |
| CO ob | | | 0.143 | 0.143 | |
| NH ob | | | 1.803 | 1.803 | |
| CN tor | | | −0.624 | 0.624 | |

[a] $\tan\theta = \frac{\partial\mu_y}{\partial S_i} \Big/ \frac{\partial\mu_x}{\partial S_i}$.

forth, by 3-21G derivatives for the complex we will mean the approximate values obtained in this way.

## RESULTS

The results for the dipole moment derivatives $\partial\mu/\partial S_i$ are given in Table III. Looking first at the 3-21G values for isolated NMA, we see that the magnitudes are generally quite large, as would be expected for such a polar molecule. While it is not surprising that the CO stretch (str) and CN str derivatives are very large, the NC str and CNC deformation (def) derivatives also turn out to be sizable. The CO in-plane bend (ib) derivative is much larger than that for CO out-of-plane bend (ob), but the converse is true of the NH ib and NH ob derivatives.

The STO-3G values for the NMA monomer agree quite closely with the 3-21G results in many cases (CC str, CN str, NH str, and CO ob), but there are large differences in others [CO str, CNC def, and CN torsion (tor)]. The tendency for STO-3G derivatives to be smaller than the 3-21G values holds in all cases except for the CN str and CO ob deriva-

tives, which, however, are virtually identical in the two bases. Although the magnitude of the STO-3G CO str derivative is much smaller, the direction of this derivative is close to the 3-21G value. Clearly, the changes in dipole derivatives with increase in basis set size are not uniform for all internal coordinates.

In going from the isolated molecule to the complex, some STO-3G derivatives increase in magnitude (CC str, CN str, CO str, NH str, NH ib, and CN tor), while the others decrease. The large increase in the NH str derivative is especially notable. A similar increase was calculated by Wójcik *et al.*[15] for the NH str derivative in the formamide dimer. Except for the CCN def derivative, there are only small changes in the directions of the $\partial\mu/\partial S_i$ on complexation; this provides some justification for our keeping the 3-21G directions unchanged when scaling from NMA to the complex. (In this scaling procedure, the CN tor derivative had to be given special treatment because of its very small magnitude in the monomer with the STO-3G set; we decided to carry over unchanged the STO-3G value for the complex to the 3-21G level.)

To summarize our results on $\partial\mu/\partial S_i$, we show in Fig. 2 the directions and relative magnitudes of the 3-21G derivatives for the complex with respect to the nine in-plane coordinates. (The vectors for the CN str and CO str derivatives have been drawn at half their lengths for convenience. All vectors are arbitrarily centered on the CO carbon.) It can be seen that the derivatives with respect to bond stretches are closely parallel to the respective bonds, and that the CO ib and NH ib derivatives are approximately perpendicular to the CO and NH bonds, respectively. The CCN def and CNC def derivatives are nearly parallel to the CN bond.

## DISCUSSION

In this section we compare our results on $\partial\mu/\partial S_i$ with experimental data; this will be done both qualitatively and quantitatively. To do so we need to transform these derivatives to the normal coordinate basis:

$$\frac{\partial\mu}{\partial Q_\alpha} = \sum_i L_{i\alpha} \frac{\partial\mu}{\partial S_i}. \tag{1}$$

$L$ is the eigenvector matrix defined by $\mathbf{S} = L\,\mathbf{Q}$. The integrated IR intensity of the $\alpha$th mode is then given by ($N$ is Avogadro's number and $c$ the velocity of light)

$$A_\alpha = \frac{N\pi}{3c^2}\left(\frac{\partial\mu}{\partial Q_\alpha}\right)^2. \tag{2}$$

The $L$ matrix is obtained from a normal mode calculation using an appropriate force field.

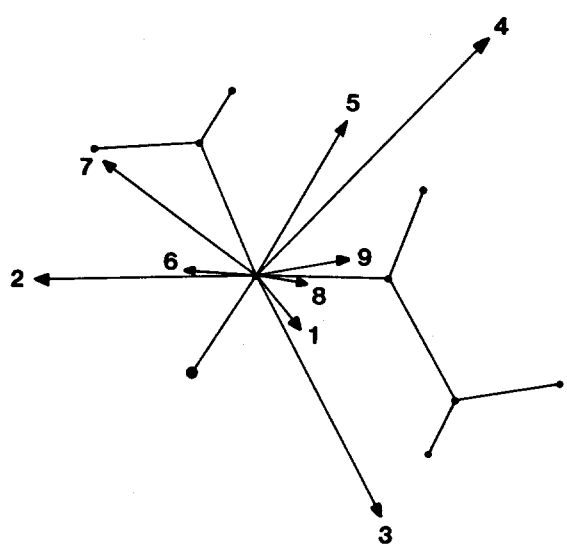


FIG. 2. 3-21G $\partial\mu/\partial S_i$ (complex) for in-plane coordinates. Numbers refer to $S_i$ of Table I. Vectors 2 and 4 are drawn at half their lengths.

### *N*-methylacetamide

Because no force field for NMA has emerged as being clearly the best based on frequency data alone, we tried several empirical force fields that give fairly good agreement between observed and calculated frequencies for NMA; these are the poly(glycine I) (PGI) force field of Dwivedi and Krimm (DK),[16] and the NMA force fields of Miyazawa *et al.* (MSM),[17] Jakeš and Krimm (JK),[18] and Rey-Lafon *et al.* (RFG).[19] We will see that the DK force field gives the best agreement with intensity data; the force constants are given in Table IV, expressed in the local symmetry coordinates of Table I. (Much better frequency agreement was obtained for NMA when an NH ob–CN tor interaction term in the PGI force field was set equal to zero.) Because we are interested mainly in the amide modes at this time, the normal mode calculations were done on NMA with the $CH_3$ groups taken to be point masses. Contributions by the methyl group coordinates to the eigenvectors for the amide modes are expected to be small and, moreover, the group moment derivatives in *n*-paraffins with respect to the $CH_3$ deformation coordinates were found empirically to be small.[4] The resulting sets of $\partial\mu/\partial Q$ are given in Table V. All the force fields yield frequencies appropriate for liquid NMA and, except in one instance, we will be comparing our results with data on NMA in the liquid and solid states. Therefore, only the derivatives obtained with the (approximate) 3-21G $\partial\mu/\partial S_i$ for the hydrogen-bonded complex are shown.

Figure 3 shows a plot of the DK values of $(\partial\mu/\partial Q)^2$ together with a spectrum of liquid NMA (capillary film). It is seen that there is good qualitative agreement: the three strong peaks (NH str, amide I and II) are followed by three peaks of decreasing intensity (amide III and the two skeletal stretches); next comes the strong amide V, and then the weak amide IV followed by a stronger amide VI, and finally a weak deformation mode. The other force fields give similar trends in the intensities, except that the JK force field predicts a stronger amide IV than amide VI.

The absolute intensity of the amide I band has been measured for NMA in dilute $CCl_4$ solution,[20] and found to be 35 000 cm mmol$^{-1}$, leading to a value for $|\partial\mu/\partial Q|$ of 2.88 $DA^{-1}u^{-1/2}$ ($u$ = atomic mass unit). The reported band position of 1691 cm$^{-1}$ indicates that this corresponds to a free CO group. If we use the monomer 3-21G $\partial\mu/\partial S_i$ values, the best agreement is obtained with the DK force field, namely 2.424 $DA^{-1}u^{-1/2}$, with the other force fields yielding

TABLE IV. Force constants for NMA in terms of coordinates of Table I.[a]

| No. | Coordinates | Value | No. | Coordinates | Value |
|---|---|---|---|---|---|
| 1 | 1,1 | 4.409 | 17 | 2,3 | 0.300 |
| 2 | 2,2 | 6.415 | 18 | 2,4 | 0.500 |
| 3 | 3,3 | 5.043 | 19 | 2,6 | 0.163 |
| 4 | 4,4 | 9.882 | 20 | 2,7 | −0.141 |
| 5 | 5,5 | 5.840 | 21 | 2,8 | 0.125 |
| 6 | 6,6 | 1.349 | 22 | 2,9 | 0.208 |
| 7 | 7,7 | 1.246 | 23 | 3,8 | 0.125 |
| 8 | 8,8 | 0.663 | 24 | 3,9 | −0.208 |
| 9 | 9,9 | 0.521 | 25 | 4,6 | −0.490 |
| 10 | 10,10 | 0.587 | 26 | 6,8 | −0.025 |
| 11 | 11,11 | 0.129 | 27 | 6,9 | 0.043 |
| 12 | 12,12 | 0.680 | 28 | 7,8 | 0.073 |
| 13 | 1,2 | 0.300 | 29 | 7,9 | −0.126 |
| 14 | 1,4 | 0.500 | 30 | 8,9 | 0.023 |
| 15 | 1,6 | 0.163 | 31 | 10,11 | 0.010 |
| 16 | 1,7 | 0.141 | 32 | 10,12 | 0.011 |

[a] Units:mdyne/Å, mdyne/rad, mdyne Å/rad$^2$.

smaller values: 2.124 (MSM), 2.028 (JK), and 1.902 (RFG). This result suggests that $(\partial\mu/\partial Q)^2$ for amide I in Fig. 3 is not grossly in error.

A more detailed look at Fig. 3 then indicates that the calculated NH str intensity may be too low. Of all the dipole derivatives, $\partial\mu/\partial r_{NH}$ is probably the most sensitive to the exact hydrogen-bonding geometry chosen in the calculation, and our choice of model may not be entirely appropriate in this respect.[9] The lower frequency ($< 700$ cm$^{-1}$) peaks are also too weak compared to the higher frequency bands, probably because the force fields are less accurate for this region where the modes are expected to be more highly mixed. All the force fields predict amide II to be stronger than amide I. The amide II band seems somewhat broader, so that its integrated intensity may indeed be larger than that of amide I. Nevertheless, while the various force fields agree closely in their amide I and II frequencies, they predict significantly different intensity ratios, from 0.81 (DK) to 0.32 (RFG). We will return to this point when we consider the PGI results.

The directions of the transition moment for the amide I, II, and III bands in crystalline NMA,[21] acetanilide,[22] *N, N'*-diacetyl hexamethylene diamine,[23] and silk fibroin[24] have been measured by various workers. Their results are shown in Table VI; the directions are measured from the CO bond in the plane of the peptide group, with positive angles toward the CC bond (clockwise in Fig. 1). The calculated directions, following this convention, of the amide I–IV modes are given in Table VII. Also shown are the separate components $L_{i\alpha}|\partial\mu/\partial S_i|$ of each $\partial\mu/\partial Q_\alpha$. (The results with the JK force field are not shown for brevity; they are very similar to the MSM results.)

With the help of Table VII, we can gain some insights into the origins of the IR intensities of the amide modes, and

TABLE V. Dipole derivatives $\partial\mu/\partial Q$ for NMA using various force fields and 3-21G $\partial\mu/\partial S$ for complex.

| | | Dwivedi and Krimm[c] | | | Miyazawa *et al.*[f] | | | Jakeš and Krimm[g] | | | Rey-Lafon *et al.*[h] | | |
|---|---|---|---|---|---|---|---|---|---|---|---|---|---|
| Mode | $\nu_{obs}$[a] | $\nu_{calc}$ | $\partial\mu/\partial Q$[b] | $\theta$[c] | $\nu_{calc}$ | $\partial\mu/\partial Q$[b] | $\theta$[c] | $\nu_{calc}$ | $\partial\mu/\partial Q$[b] | $\theta$[c] | $\nu_{calc}$ | $\partial\mu/\partial Q$[b] | $\theta$[c] |
| 1 NH str | 3236S[d] | 3254 | 2.101 | 63 | | | | 3294 | 2.105 | 63 | 3305 | 2.114 | 63 |
| 2 Amide I | 1653S | 1637 | 2.892 | 41 | 1650 | 2.476 | 49 | 1631 | 2.317 | 51 | 1655 | 2.109 | 77 |
| 3 Amide II | 1567S | 1510 | 3.215 | −11 | 1516 | 3.388 | 0 | 1519 | 3.544 | −1 | 1564 | 3.711 | 6 |
| 4 Amide III | 1299M | 1273 | 1.027 | −78 | 1286 | 1.445 | −59 | 1305 | 1.224 | −70 | 1343 | 1.019 | −39 |
| 5 NC str | 1096W | 1070 | 0.647 | −64 | 999 | 0.729 | −79 | 1086 | 0.821 | −73 | 1097 | 0.648 | −66 |
| 6 CN str,CC str | 881W | 900 | 0.163 | 61 | 945 | 0.428 | −10 | 953 | 0.333 | 79 | 947 | 0.593 | 48 |
| 7 Amide V | 725S | 730 | 1.443 | Z | | | | 746 | 1.457 | Z | 745 | 1.526 | Z |
| 8 Amide IV | 627W | 635 | 0.220 | −69 | 600 | 0.360 | −42 | 679 | 0.232 | −79 | 600 | 0.334 | −38 |
| 9 Amide VI | 600M | 640 | 0.467 | Z | | | | 578 | 0.003 | Z | 604 | 0.674 | Z |
| 10 CCN def | 436W | 498 | 0.338 | 59 | 431 | 0.325 | 87 | 489 | 0.345 | 68 | 464 | 0.346 | 79 |
| 11 CNC def | 289 | 271 | 0.239 | −29 | 263 | 0.296 | −16 | 320 | 0.160 | −17 | 315 | 0.321 | −17 |
| 12 Amide VII | 206 | 225 | 0.736 | Z | | | | 182 | 0.849 | Z | 108 | 0.249 | Z |

[a] In cm$^{-1}$. S = strong, M = medium, W = weak. T. Miyazawa, T. Shimanouchi, and S. I. Mizushima, J. Chem. Phys. **24**, 408 (1956); **29**, 611 (1958).
[b] In D/A $u^{1/2}$.
[c] Angle in degrees to $X$ axis (CN bond) in $XY$ plane. $\theta > 0$: counterclockwise from $X$ in Fig. 1.
[d] Unperturbed value. T. Miyazawa, J. Mol. Spectrosc. **4**, 168 (1960).
[e] Reference 16.
[f] Reference 17.
[g] Reference 18.
[h] Reference 19.

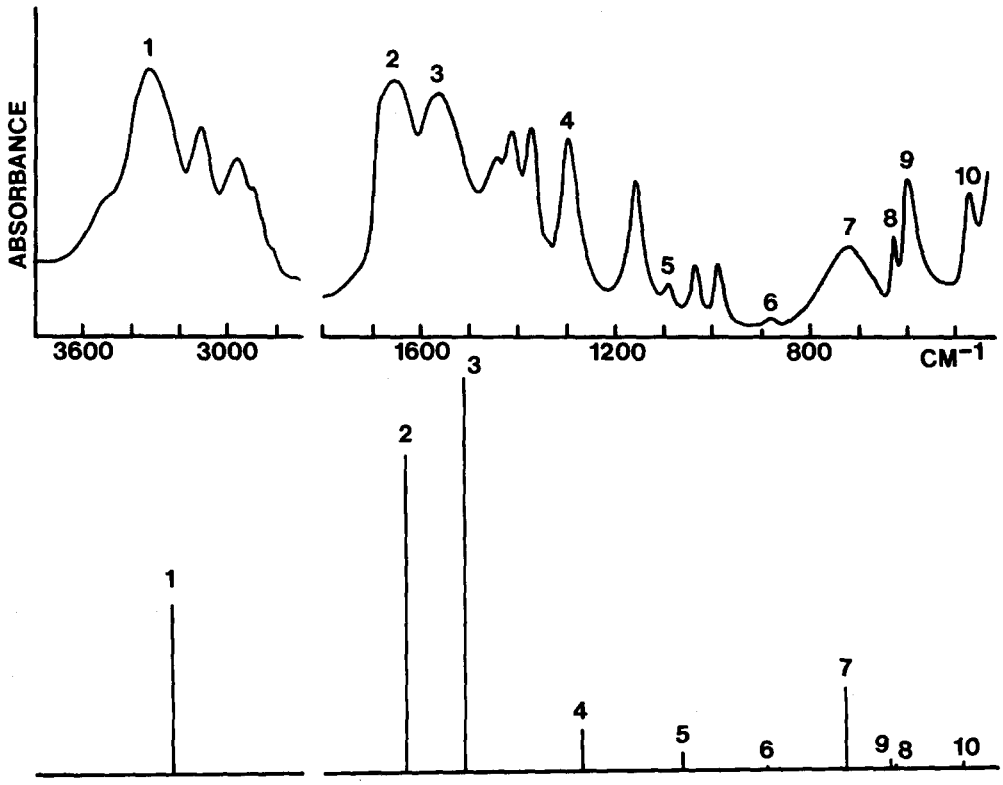


FIG. 3. Top: Infrared spectrum of liquid *N*-methylacetamide (capillary film). Bottom: Plot of $(\partial\mu/\partial Q)^2$ for *N*-methylacetamide using the Dwivedi–Krimm force field (Ref. 16) and 3-21G $\partial\mu/\partial S$ (complex). Numbers on peaks correspond to numbered modes in Table V.

TABLE VI. Measured directions of transition moment for amide bands.[a]

| | Amide I | Amide II | Amide III | Reference |
|---|---|---|---|---|
| *N*-methylacetamide | + 15° to 25° | + 73° or − 37° | + 96° or − 60° | 21 |
| Acetanilide | + 22°(± 2) | + 72° or − 57° | | 22 |
| *N, N'*-diacetyl hexamethylene diamine | + 17° | + 68°, + 77° (doublet) | | 23 |
| Silk fibroin | + 19° | | | 24 |

[a] Measured from the CO bond direction in plane of peptide group (positive: towards CC bond; negative: towards CN bond).

TABLE VII. Contributions $L_{i\alpha}\left|\frac{\partial\mu}{\partial S_i}\right|$ (in D/A $u^{1/2}$) to $\partial\mu/\partial Q_\alpha$ for amide I, II, III, and IV modes of NMA using various force fields and 3-21G $\partial\mu/\partial S_i$ for complex.

| | Amide I | | | Amide II | | | Amide III | | | Amide IV | | |
|---|---|---|---|---|---|---|---|---|---|---|---|---|
| | DK[a] | MSM[b] | RFG[c] | DK | MSM | RFG | DK | MSM | RFG | DK | MSM | RFG |
| CC str | 0.10 | 0.10 | 0.18 | 0.13 | 0.06 | 0.05 | − 0.14 | − 0.16 | − 0.13 | 0.09 | 0.09 | 0.11 |
| CN str | 0.81 | 0.69 | 0.09 | − 1.28 | − 1.25 | − 1.46 | 0.69 | 1.03 | 0.82 | − 0.10 | 0.05 | 0.13 |
| NC str | − 0.02 | 0.05 | 0.16 | 0.38 | 0.38 | 0.32 | − 0.21 | − 0.20 | − 0.25 | 0.11 | 0.14 | 0.12 |
| CO str | − 2.57 | − 2.46 | − 2.28 | − 0.07 | 0.50 | 1.01 | 0.29 | 0.66 | − 0.28 | 0.02 | 0.10 | 0.12 |
| NH str | 0.02 | − 0.03 | 0.03 | 0.00 | 0.01 | − 0.02 | − 0.01 | − 0.01 | − 0.01 | − 0.01 | − 0.01 | − 0.01 |
| CCN def | − 0.27 | − 0.27 | − 0.27 | − 0.04 | 0.02 | 0.09 | 0.04 | 0.04 | − 0.01 | − 0.01 | 0.00 | − 0.03 |
| CO ib | 0.02 | − 0.01 | − 0.41 | − 0.71 | − 0.46 | − 0.49 | 0.60 | 0.68 | 0.67 | 0.61 | 0.64 | 0.56 |
| CNC def | − 0.12 | − 0.12 | − 0.14 | − 0.03 | 0.02 | 0.06 | 0.07 | 0.04 | 0.06 | 0.10 | 0.09 | 0.08 |
| NH ib | 0.19 | 0.51 | 0.51 | 1.10 | 1.24 | 1.02 | 0.96 | 0.62 | 0.92 | 0.08 | 0.03 | 0.01 |
| Total | 2.89 | 2.48 | 2.11 | 3.22 | 3.39 | 3.71 | 1.03 | 1.45 | 1.02 | 0.22 | 0.36 | 0.33 |
| Angle from CO(°) | 17 | 9 | − 19 | 69 | 58 | 52 | 137 | 118 | 97 | 128 | 100 | 96 |

[a] Reference 16.
[b] Reference 17.
[c] Reference 19.

into the deficiencies of each force field.

Looking at the results for amide I, we see that the direction of $\partial\mu/\partial Q$ calculated with the DK force field ( + 17°) is in virtually exact agreement with experiment, whereas the RFG force field gives a vector on the other side of the CO bond. For each force field, the CO str contribution is nearly equal to $|\partial\mu/\partial Q|$ itself. However, since a pure CO str mode would have a transition moment oriented at + 11° to CO (see Table III), mixing with other coordinates is required to cause a deviation from this angle. For both the DK and MSM results, there is a large contribution from CN str; this is out of phase with the CO str component and therefore adds to the latter, causing a rotation of $\partial\mu/\partial Q$ toward the CC bond (see Fig. 2). In the MSM results, however, an NH ib component in phase with CN str almost exactly cancels the latter's contribution, resulting in insufficient rotation of $\partial\mu/\partial Q$. With the RFG force field, the CN str component is negligible and the NH ib component subtracts from the CO str; a significant CO ib component further causes the rotation of $\partial\mu/\partial Q$ toward the CN bond. Thus, the intensity of the amide I mode arises mainly from CO str and CN str, and the particular merit of the DK force field compared to the others is that it yields a large CN str contribution, together with small NH ib and CO ib components.

Turning to the amide II results, we again find the DK direction of $\partial\mu/\partial Q$ ( + 69°) to be in excellent agreement with experiment. (Due to a sign indeterminacy, Bradbury and Elliott[21] derived two values for the transition moment in NMA, + 73° and − 37°. They concluded that the former value is correct in view of Sandeman's[23] data. Our results confirm their conclusion.) All three force fields agree in showing that the strong amide II intensity is due largely to the out-of-phase vibration of CN str and NH ib. These two components by themselves would yield a transition moment approximately along the CN bond (at + 58.2°). Sizable CO ib and NC str contributions with the DK force field rotate $\partial\mu/\partial Q$ to a larger angle. With the other two force fields, the CO ib contribution is smaller, and a large CO str component serves to rotate $\partial\mu/\partial Q$ back toward CO.

The much lower intensity of amide III compared to amide II is seen to be due to the in-phase vibration of CN str and NH ib. The sign indeterminacy in the experimental transition moment direction [ + 96° or − 60°( + 120°)] makes it impossible to say which force field is best in this case since each gives a direction consistent with one of the two measured angles. All three force fields agree in showing that, because of the approximate cancellation of the CN str and and NH ib contributions, $\partial\mu/\partial Q$ for amide III is determined mainly by CO ib and, according to the MSM results, CO str.

The amide IV band also owes its intensity to CO ib, but unlike the amide III, the smaller CC str and NC str components are in phase with CO ib, leading to subtraction instead of reinforcement. Hence the very low intensity of amide IV. Clearly the precise mixing of numerous coordinates in this mode is especially important, making it difficult to derive an accurate eigenvector empirically. The direction of $\partial\mu/\partial Q$ is predicted by each force field to be nearly the same as for amide III.

The amide V, VI, and VII modes involve the NH ob, CO ob, and CN tor coordinates, but because of the small $\partial\mu/\partial S$ for CO ob, the intensities of these modes depend on the other two coordinates. (Our discussion will be based on the DK results; the MSM force field is only for the in-plane vibrations, and we cannot be completely certain of how RFG defined their out-of-plane bending and torsional coordinates.) The amide V has 57% of its potential energy in CN tor and 38% in NH ob, but the contributions to $\partial\mu/\partial Q$ are 0.32 and 1.75 $DA^{-1}u^{-1/2}$, respectively, in opposite directions. This difference in the character of a mode as measured by its potential energy distribution (PED) and by the contributions to its intensity shows that it may be useful to characterize a mode not only by its eigenvector (Cartesian and internal) and PED, but also by its intensity distribution. For the amide VI, CO ob accounts for 88% of the potential energy but contributes only 0.086 $DA^{-1}u^{-1/2}$ to the $\partial\mu/\partial Q$ of 0.467 $DA^{-1}u^{-1/2}$. The NH ob and CN tor contributions are in the same direction for this mode; the JK force field, however, gives these components in opposite directions, resulting in the very low predicted intensity. The amide VII is another strong mixing of NH ob (60%) and CN tor (31%), but owes its intensity almost entirely to NH ob (0.673 of a total of 0.736 $DA^{-1}u^{-1/2}$). Finally, we should point out that because of the relatively simple mixing in the amide VI mode, it is not clear why our predicted intensity (peak 9 in Fig. 3) seems rather low. Possibly, the NH ob contribution should be larger, or $\partial\mu/\partial S$ for CO ob is significantly underestimated. It has been found that in computing out-of-plane force constants in formamide,[8] a larger basis set was necessary than for the in-plane force constants. We calculated the dipole moment derivative with respect to CO ob in formaldehyde, and got a value of 0.256 D/rad with the 3-21G basis compared to an experimental value of 0.293 D/rad.[25] Whether the CO ob derivative in NMA is of comparable accuracy we cannot be sure at present.

### Poly(glycine I)

We now discuss the transferring of the derivatives $\partial\mu/\partial S_i$ to PGI. The transferability of group moment derivatives depends on two assumptions. First, analogous to the bond moment model, we neglect the effects on $\partial\mu/\partial S_i$ of changes in charge distributions when a group is in different molecules; also neglected, in a zero-order group moment model, are the cross derivatives involving different groups, $(\partial\mu_{g'}/\partial S_i^g)(g \neq g')$. (Note, however, that a group moment derivative implicitly includes some first-order bond moment derivatives.) The second asusmption involves the fact that a derivative $\partial\mu/\partial S_i$ cannot be strictly transferable because the internal coordinate displacement $S_i$ is different in different molecules and isotopic species owing to the need for a small compensating rotation of the molecule to satisfy the Eckart conditions.[26] For a polar molecule this rotation results in a contribution to the dipole derivative that is proportional to the static moment. Because this rotational correction is also inversely proportional to the moments of inertia, as a first approximation it can be neglected in the case of peptides, especially in view of the large magnitudes of the dipole derivatives. (This neglect of rotational corrections is also im-

TABLE VIII. Dipole derivatives $\partial\mu/\partial Q$ for poly(glycine I).

| Mode | $\nu_{obs}$ [a] | $\nu_{calc}$ [b] | Symm | $\frac{\partial\mu}{\partial Q}$ [c] | $\theta$ [d] | Projected $\partial\mu/\partial Q$ |
|---|---|---|---|---|---|---|
| 1 NH str | 3272S | 3271 | $B_u$ | 2.130 | 59 | 2.130 |
| 2 Amide I | 1685M | 1689 | $A_u$ | 3.144 | 34 | 1.280 |
| 3 Amide I | 1636S | 1643 | $B_u$ | 3.065 | 30 | 2.703 |
| 4 Amide II | ... | 1572 | $B_u$ | 2.617 | −24 | 0.892 |
| 5 Amide II | 1517S | 1515 | $A_u$ | 2.764 | −21 | 2.571 |
| 6 Amide III | 1295W | 1286 | $B_u$ | 1.417 | −83 | 1.143 |
| 7 Amide III | 1214W | 1212 | $A_u$ | 0.956 | −54 | 0.813 |
| 8 $NC^{\alpha}$ str | 1016M | 1014 | $B_u$ | 0.686 | 79 | 0.458 |
| 9 $C^{\alpha}C$ str,CN str | 888W | 890 | $B_u$ | 0.226 | 67 | 0.216 |
| 10 Amide V | 708S | 718 | $B_u$ | 0.733 | 9 | 0.666 |
| 11 Amide IV | 628W | 629 | $A_u$ | 0.578 | −88 | 0.301 |
| 12 Amide VI | 614M | 621 | $B_u$ | 0.923 | 50 | 0.887 |
| 13 Amide VI | 589M | 579 | $A_u$ | 0.596 | −55 | 0.028 |
| 14 Skeletal def | 321W | 320 | $B_u$ | 0.526 | −79 | 0.223 |
| 15 Skeletal def | 285W | 290 | $A_u$ | 0.139 | 81 | 0.040 |
| 16 Skeletal def | 217W | 226 | $A_u$ | 0.183 | −31 | 0.157 |

[a] In $cm^{-1}$. S = strong, M = medium, W = weak.
[b] Reference 16.
[c] In D/A $u^{1/2}$.
[d] Angle in degrees to $X$ axis (CN bond) in $XY$ plane. $\theta > 0$: counterclockwise from $X$ in Fig. 1.

plicit in our use of a six-body model of NMA to obtain the $L$ matrix.) One of the main advantages of the bond moment model, of course, is the isotopic invariance of bond moment parameters,[26] but as we mentioned in the Introduction, this model is difficult to apply to peptides.

The dipole derivatives $\partial\mu/\partial Q$ for PGI using the 3-21G $\partial\mu/\partial S_i$ (complex) and the eigenvectors of DK[16] are given in Table VIII. Except for the $B_u$ amide II vibration calculated at 1572 $cm^{-1}$, only those modes for which experimental assignments are available are shown. The $A_u$ modes, $\nu(0, \pi)$, have polarization along the chain direction, and the $B_u$ modes, $\nu(\pi, 0)$, are polarized perpendicular to the chain axis; we have therefore also shown the values of $\partial\mu/\partial Q$ for each mode projected accordingly. The relative intensities, as given by the squares of these projected values of $\partial\mu/\partial Q$, are plotted in Fig. 4 together with a spectrum of PGI in the solid state (in KBr). (There is a small amount of PGII impurity, but as can be checked against the PGI spectrum of Suzuki *et al.*,[27] this should not affect our conclusions.)

Because of the bad overlaps in the region below 1500

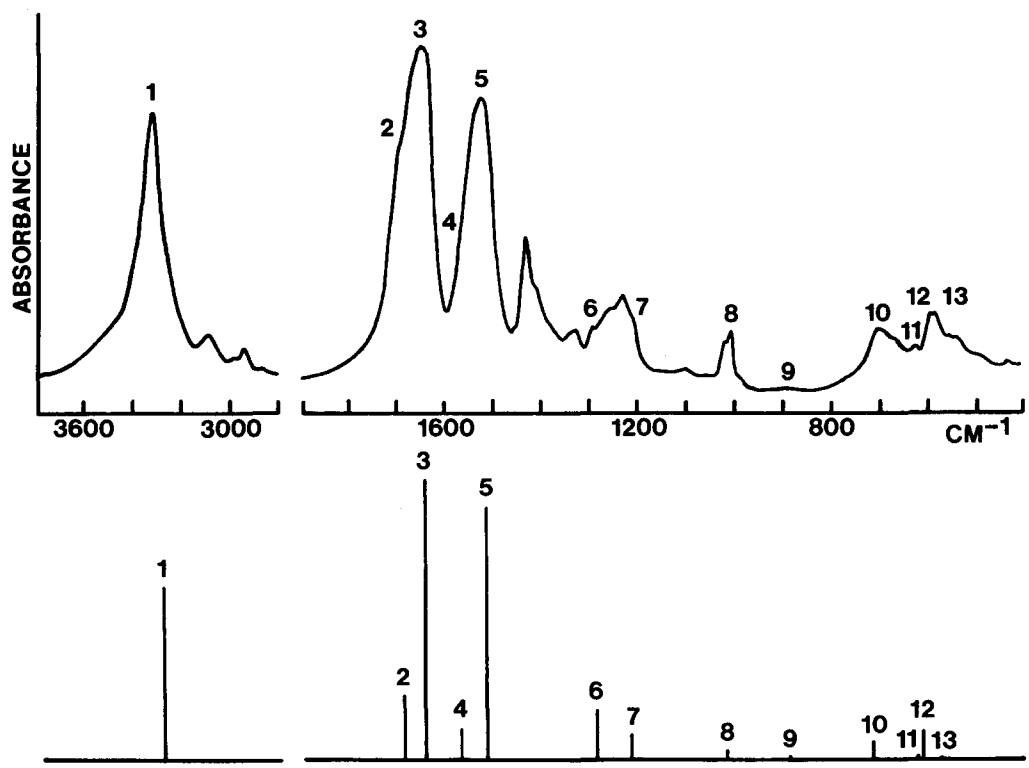


FIG. 4. Top: Infrared spectrum of solid poly(glycine I) (KBr pellet). Bottom: Plot of projected $(\partial\mu/\partial Q)^2$ for poly(glycine I) using the Dwivedi–Krimm force field (Ref. 16) and 3-21G $\partial\mu/\partial S$ (complex). Numbers on peaks correspond to numbered modes in Table VIII.

$cm^{-1}$, it is difficult to make a meaningful comparison of the calculated and observed band intensities. It is also possible that some assignments should be reversed from $A_u$ to $B_u$, and vice versa. For the NH str and amide I and II modes, the calculated peaks agree very well with the observed relative band intensities. Absolute intensities of amide I and II bands have been measured by Chirgadze *et al.*[28] for various polypeptides in solution. The values of $|\partial\mu/\partial Q|$ for the amide I mode of random coil structures implied by these intensities range from 2.75 to 3.47 $DA^{-1}u^{-1/2}$, while a value for amide II of 2.84 $DA^{-1}u^{-1/2}$ can be derived from their results. These values are expected to be representative of the transition moments of an individual peptide group, and can be compared to our calculated unprojected values of $\partial\mu/\partial Q$. The agreement is seen to be good for both amide I and II. In particular, the amide I intensity measured for silk fibroin of *B. mori*, which has a high glycine content, yields a $|\partial\mu/\partial Q|$ of 3.15 $DA^{-1}u^{-1/2}$, in excellent agreement with our calculations. (This particular measurement was made in $D_2O$ solution; however, the amide I eigenvector for *N*-deuterated PGI is negligibly different, except for a further decrease in the very small NH ib contribution.)

Chirgadze *et al.*[28] also measured the amide I and II band intensities for $\beta$-sheet structures. These data should be compared with our projected $\partial\mu/\partial Q$. The ranges of the values of $|\partial\mu/\partial Q|$ derived from their results for the amide I components are as follows: $\nu(0,\pi)$ — 0.97 to 1.54 $DA^{-1}u^{-1/2}$; $\nu(\pi,0)$ — 3.34 to 3.80 $DA^{-1}u^{-1/2}$. For the amide II components, the values of $|\partial\mu/\partial Q|$ obtained were 1.09 [$\nu(\pi,0)$] and 2.43 $DA^{-1}u^{-1/2}$ [$\nu(0,\pi)$]. Our projected values of $|\partial\mu/\partial Q|$ agree very well with these data; the large absolute error for the amide I $\nu(\pi,0)$ component represents a discrepancy of about 20% and is therefore still acceptable. It should be noted that the $\beta$-sheet intensity measurements[28] were made with solutions containing mixtures of random coil and $\beta$-sheet structures. To obtain the intensity parameters for the ordered form, it was necessary to subtract the contributions of the random coil component. The $\beta$-sheet intensity parameters may therefore be expected to be subject to larger uncertainties than those for the random coil.

Besides the absolute intensity, another independent measure of $\partial\mu/\partial Q$ derives from transition dipole interaction or coupling (TDC) between peptide groups.[29] Analysis of the various components of the amide I mode in PGI showed that the factor group splittings could be explained on the basis of TDC if one assumed a $\partial\mu/\partial Q$ of 3.44 $DA^{-1}u^{-1/2}$ oriented at + 20° to the CO bond. Similarly, the amide II splittings could be fitted by a $\partial\mu/\partial Q$ of 2.43 $DA^{-1}u^{-1/2}$ at + 68° to CO. In these TDC analyses, the transition moment directions were chosen to be consistent with IR dichroism measurements (Table VI). Our calculated directions for the amide I and II transition moments in PGI are given in Table IX. It can be seen that our calculated $\partial\mu/\partial Q$ are consistent in both magnitude and direction with intensity and TDC results, as well as with dichroism data.

We may therefore have confidence in the projected values of $(\partial\mu/\partial Q)^2$ for amide I and II in Fig. 4. It is apparent then that the NH str band is much better fitted in PGI than is the case in NMA, indicating that our hydrogen bonding model may be more representative of the situation in PGI, where the narrower and higher frequency NH str band suggests a weaker hydrogen bond, and where linearity is strongly suggested.[30] Because of the importance of the amide I and II modes in conformational studies of polypeptides and proteins, it is especially interesting that the intensities of these modes are fitted very well. Thus, the group moment parameters $\partial\mu/\partial S_i$ determined for NMA give even better results when transferred to PGI. This can be explained by the fact that the eigenvectors for PGI are obtained with a refined force field. With the help of Table IX, which shows the separate contributions $L_{i\alpha}|\partial\mu/\partial S_i|$ to $\partial\mu/\partial Q$ for amide I, II, and III, we can try to understand why the fit is better for PGI.

The decomposition of $\partial\mu/\partial Q$ for amide I is very similar for the $A_u$ and $B_u$ modes. Comparing with the DK results for NMA, we see that the larger magnitude of $\partial\mu/\partial Q$ in PGI, and the larger angle from CO are due to the larger CN str and smaller NH ib contributions. Moreover, there is a new sizable CO ib component which, unlike in the RFG results, is out of phase with CO str; this difference in phase helps the rotation of $\partial\mu/\partial Q$ toward the $C^\alpha C$ bond instead of toward the CN bond.

The amide II intensity decomposition is also very simi-

TABLE IX. Contributions $L_{i\alpha}\left|\frac{\partial\mu}{\partial S_i}\right|$ (in D/A $u^{1/2}$) to $\partial\mu/\partial Q_\alpha$ for amide I, II, and III modes of poly(glycine I).

| | Amide I | | Amide II | | Amide III | |
|---|---|---|---|---|---|---|
| | $A_u$ | $B_u$ | $A_u$ | $B_u$ | $A_u$ | $B_u$ |
| CC str | − 0.06 | − 0.04 | 0.17 | 0.17 | − 0.03 | − 0.14 |
| CN str | − 1.05 | − 1.09 | − 1.11 | − 0.83 | 0.61 | 0.61 |
| NC str | − 0.01 | 0.16 | 0.27 | 0.43 | − 0.64 | − 0.36 |
| CO str | 2.47 | 2.38 | − 0.54 | − 0.62 | − 0.01 | 0.62 |
| NH str | − 0.03 | − 0.03 | − 0.01 | − 0.01 | − 0.01 | − 0.01 |
| CCN def | 0.28 | 0.27 | − 0.10 | − 0.10 | 0.13 | 0.03 |
| CO ib | − 0.16 | − 0.21 | − 0.79 | − 0.59 | 0.18 | 0.71 |
| CNC def | 0.12 | 0.11 | − 0.09 | − 0.03 | 0.05 | 0.08 |
| NH ib | − 0.05 | − 0.08 | 0.97 | 1.15 | 0.63 | 0.82 |
| CO ob | 0.00 | 0.00 | 0.00 | 0.00 | 0.00 | 0.00 |
| NH ob | 0.02 | − 0.05 | − 0.07 | − 0.07 | 0.10 | − 0.06 |
| CN tor | 0.01 | − 0.01 | 0.00 | − 0.02 | 0.04 | 0.00 |
| Total | 3.14 | 3.06 | 2.76 | 2.62 | 0.96 | 1.42 |
| Angle from CO(°) | 24 | 29 | 79 | 82 | 113 | 141 |

lar to the DK results for NMA, with the chief difference being a significant CO str contribution which is in phase with CN str and out of phase with NH ib, thus tending to subtract from the latter two contributions. The result is a smaller $\partial\mu/\partial Q$ for amide II in PGI. By contrast, the MSM and RFG (and also JK) force fields give an amide II in NMA in which the CO str is out of phase with CN str.

Thus, the absolute and relative magnitudes and directions of the amide I and II transition moments are the result of a rather fine balance among the contributions from CO str, CN str, NH ib, and CO ib. In NMA we have seen that different force fields, all of which give good frequency agreement for amide I and II, can yield significantly different eigenvectors and, therefore, transition moment parameters. All these force fields have been shown to give good *N*-deuteration shifts, but the significant difference is that the DK force field was also refined to fit $^{15}N$ isotope shifts in PGI. As Abe and Krimm[10] pointed out, the difference between the CO str and CN str force constants is sensitive mainly to the $^{15}N$ shifts of the amide I and II modes. These two force constants determine the mixing of CO str and CN str in amide I and II. For instance, if we adjust $f_2$ in Table IV from 6.415 to 6.8 mdyne/Å, the amide I and II frequencies in NMA improve slightly to 1645 and 1526 $cm^{-1}$, but the eigenvectors change sufficiently to give nearly equal intensities for amide I and II ($|\partial\mu/\partial Q| = 3.05$ and $3.07\ DA^{-1}u^{-1/2}$, respectively). Adjustment of $f_9$ (to 0.57), $f_{22}$ (to 0.15), and $f_{23}$ (to $-0.3$) would give even better frequency agreement (1662 and 1569 $cm^{-1}$), but the relative intensity of amide I to amide II decreases further, from 0.81 to 0.79.

Thus, we conclude that the optimization of the DK force field for $^{15}N$ shifts as well as deuteration shifts in PGI results in more correct eigenvectors not only for PGI but also for NMA. The additional improvement in the calculated intensities of amide I and II in PGI occurs because of the use of TDC force constants, leading to better frequency agreement and stronger mixing of CO str and CN str in these modes. As confirmation of this last point, the PGI eigenvectors of Abe and Krimm,[10] which were obtained with $^{15}N$ shifts but without TDC terms, yield unprojected $|\partial\mu/\partial Q|$ values of 2.904 and $3.059\ DA^{-1}u^{-1/2}$ for amide I and II, respectively, in decidedly poorer agreement with experiment than the DK results. (The recent calculation of PGI by Stepanyan and Gribov[2] apparently also does not include TDC terms and is unable to reproduce the large amide I splitting. The highest frequency component is predicted to be the most intense, in contradiction to observation. Only relative (unprojected?) intensities are reported in their paper, so we cannot compare values of $\partial\mu/\partial Q$ in more detail.)

## CONCLUSIONS

In this paper we have demonstrated one approach by which infrared intensities can be studied in complex molecules and polymers. We have shown that *ab initio* calculations at the Hartree–Fock level with a relatively small basis set are capable of giving dipole moment derivatives that are quantitatively correct.

The group moment derivatives calculated for *N*-methylacetamide were transferred to poly(glycine I) where, because more reliable eigenvectors were available, the agreement with observations was even better in the case of the important amide I and II modes. By examining the separate contributions of each internal coordinate to the total intensity, we have been able to understand in more detail the origins of the IR intensities of the amide modes. These results provide a basis for using IR intensities in structural studies of peptides, polypeptides, and proteins, as we will try to show in future work.

Our results on NMA and PGI have shown the effectiveness and transferability of the empirical PGI force field of Dwivedi and Krimm,[16] and the importance of including transition dipole interaction force constants for the amide I and II modes. The significant differences in relative and absolute intensities obtained with different force fields, all of which give good frequency agreement, show that intensity data can be used in refining empirical force fields or in choosing between different sets. In complex molecules, *ab initio* group moment derivatives may be used for this purpose.

## ACKNOWLEDGMENTS

This research was supported by National Science Foundation Grants PCM-8214064 and DMR-8303610. One of us (T.C.C.) is indebted to the Macromolecular Research Center for postdoctoral fellowship support.

*Note added in proof*: In a paper [L. R. Schroeder and S. L. Cooper, J. Appl. Phys. **47**, 4310 (1976)] that came to our attention only recently, the absolute intensities of the NH str bands in several nylons were measured. These data yield values for $|\partial\mu/\partial Q|$ of 1.69 to 2.18 $D/Au^{1/2}$ for hydrogen-bonded NH groups, and 1.03 $D/Au^{1/2}$ for free NH groups. These compare very well with our calculated $|\partial\mu/\partial Q|$ for PGI:2.130 $D/Au^{1/2}$ (bonded) and 0.927 $D/Au^{1/2}$ (free).

[1] *Vibrational Intensities in Infrared and Raman Spectroscopy*, edited by W. Person and G. Zerbi (Elsevier, Amsterdam, 1982).
[2] S. A. Stepanyan and L. A. Gribov, Opt. Spectrosc. **47**, 165 (1979).
[3] S. Krimm, Biopolymers **22**, 217 (1983).
[4] R. G. Snyder, J. Chem. Phys. **42**, 1744 (1965).
[5] M. Kitano, T. Fukuyama, and K. Kuchitsu, Bull. Chem. Soc. Jpn. **46**, 384 (1973).
[6] R. B. Corey and L. Pauling, Proc. R. Soc. London Ser. B **141**, 10 (1953).
[7] G. Fogarasi, P. Pulay, F. Torok, and J. E. Boggs, J. Mol. Struct. **57**, 259 (1979).
[8] Y. Sugawara, Y. Hamada, A. Hirakawa, M. Tsuboi, S. Kato, and K. Morokuma, Chem. Phys. **50**, 105 (1980).
[9] R. Taylor, O. Kennard, and W. Versichel, J. Am. Chem. Soc. **105**, 5761 (1983).
[10] Y. Abe and S. Krimm, Biopolymers **11**, 1817 (1972).
[11] P. Pulay, G. Fogarasi, F. Pang, and J. E. Boggs, J. Am. Chem. Soc. **101**, 2550 (1979).
[12] C. M. Cook, Quantum Chem. Prog. Exchange **13**, 391 (1981).
[13] W. J. Hehre, R. Ditchfield, and J. A. Pople, J. Chem. Phys. **56**, 2257 (1972).
[14] J. S. Binkley, J. A. Pople, and W. J. Hehre, J. Am. Chem. Soc. **102**, 939 (1980).
[15] M. J. Wojcik, A. Y. Hirakawa, M. Tsuboi, S. Kato, and K. Morokuma, Chem. Phys. Lett. **100**, 523 (1983).
[16] A. M. Dwivedi and S. Krimm, Macromolecules **15**, 177 (1982).
[17] T. Miyazawa, T. Shimanouchi, and S. Mizushima, J. Chem. Phys. **29**, 611 (1958).

[18]J. Jakeš and S. Krimm, Spectrochim. Acta Part A **27**, 19 (1971).
[19]M. Rey-Lafon, M. T. Forel, and C. Garrigou-Lagrange, Spectrochim. Acta Part A **29**, 471 (1973).
[20]V. Venkata Chalapathi and K. Venkata Ramiah, J. Mol. Spectrosc. **26**, 444 (1968).
[21]E. M. Bradbury and A. Elliott, Spectrochim. Acta **19**, 995 (1963).
[22]N. B. Abbott and A. Elliott, Proc. R. Soc. London Ser. A **234**, 247 (1956).
[23]I. Sandeman, Proc. R. Soc. London Ser. A **232**, 105 (1955).
[24]E. Suzuki, Spectrochim. Acta Part A **23**, 2302 (1967).
[25]T. Nakanaga, S. Kondo, and S. Saeki, J. Chem. Phys. **76**, 3860 (1982).
[26]M. Gussoni, in *Advances in Infrared and Raman Spectroscopy*, edited by R. J. H. Clark and R. E. Hester (Heyden, London, 1980), Vol. 6.
[27]S. Suzuki, Y. Iwashita, T. Shimanouchi, and M. Tsuboi, Biopolymers **4**, 337 (1966).
[28]Yu. N. Chirgadze, B. V. Shestopalov, and S. Yu. Venyaminov, Biopolymers **12**, 1337 (1973).
[29]T. C. Cheam and S. Krimm, Chem. Phys. Lett. **107**, 613 (1984).
[30]W. H. Moore and S. Krimm, Biopolymers **15**, 2439 (1976).